ELSEVIER

Journal of Photochemistry and Photobiology A: Chemistry 120 (1999) 93–103

Journal of Photochemistry and Photobiology A:Chemistry

Sensitized proton formation using lipophilic substituted iodonium salts☆

Uwe Müller*, Inge Zücker

Institut für Organische Chemie der Martin-Luther-Universität Halle-Wittenberg, Geusaer Straße, D-06217 Merseburg, Germany

Received 11 September 1998; accepted 9 October 1998

Abstract

Iodonium salt/sensitizer combinations are excellent initiators of the photoinduced cationic crosslinking. Our results shows that the well-known kinetics of the sensitized photoinduced proton formation of iodonium salts must be extended by a CT-complex formation and by the photochemistry of this complex. Moreover, the sensitized photochemistry of the lipophilic iodonium salts differ from the unsubstituted product.

The observed nonequivalence of the quantum yield of proton formation and quantum yield of sensitizer photolysis results presumably from the self-solvatisation of the iodonium salts. Moreover, the nonequivalence of the quantum yields is combined with the emergence of a CT complex.

Keywords: Liphophilic iodonium salts; Electron transfer; Proton formation; Polymerization initiators

1. Introduction

Iodonium salt/sensitizer combinations are important initiators of cationic photopolymerizations [1]. Using fluorescence and laser flash techniques one can show that iodonium salts react efficiently with photoexcited singlet and triplet states of several sensitizers [1–3]. As has been shown, under these circumstances the quenching mechanism is an electron transfer to give the radical cation of the sensitizer and the neutral radical of the onium salt if this is thermodynamically feasible; see Scheme 1, where diphenylanthracene (DPA) was used as sensitizer and an iodonium salt $I^{\oplus}$ was used as onium compound. The initiating species of such initiator system, the protons, are formed in a consecutive reaction from the cation radical of the sensitizer. Moreover, the proton formation is combined by the consumption of the sensitizer.

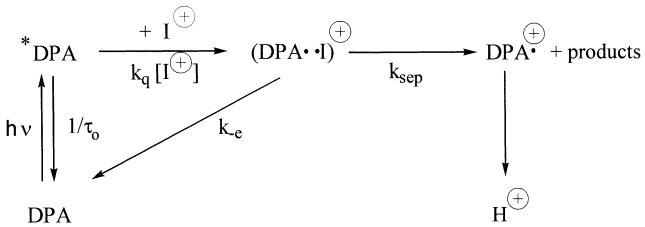

Scheme 1.

In this work, we therefore study the proton formation of lipophilic iodonium salts $I_{(1)}$–$I_{(3)}$ with DPA as sensitizer in solvents with different polarity (acetonitrile, ε=35.94; methanol, ε=32.66; dimethoxymethane (DME), ε=7.20; dioxane, ε=2.21; *n*-heptane, ε=1.92 [4]). With the exception of dioxane all solvents use similar viscosities (η=0.345 (CH_3CN); 0.593 (CH_3OH); 0.455 (DME); 1.439 (dioxane); 0.418 (*n*-heptane); all values in mPa s [4]). The lipophilic iodonium compounds investigated are shown in Scheme 2 with their abbreviations adopted in this work; if not marked, they were employed as their $SbF_6^{\ominus}$-salts, which eliminates complications caused by participation of nucleophilic and/or oxidizable anions in these reactions. Additionally, the sensitized proton formation from $Ph_2I^{\oplus}$ $SbF_6^{\ominus}$ ($I_{(4)}$) was studied to compare the results in these solvents with those from the lipophilic products $I_{(1)}$–$I_{(3)}$. The photochemistry of the sensitized proton formation was investigated in three steps, namely fluorescence quenching, sensitizer decay, and proton formation. Mostly, the photolysis was carried out under air to eliminate the secondary induced proton formation [5,6]. Moreover, measurements under inert conditions, and under oxygen were carried out to study the influence of oxygen on the sensitized proton formation.

*Corresponding author.

☆Presented at the conference "Reduce Coatings and Inks: Coating and Performance" in Harrogate, 1998.

1010-6030/99/$ – see front matter
PII: S1010-6030(98)00419-5

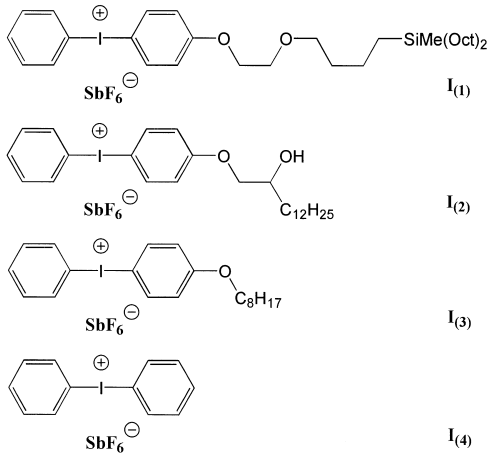

Scheme 2.

2. Experimental part

All lipophilic iodonium salts were experimental or commercial products ($I_{(1)}$ – Wacker-Chemie, $I_{(2)}$ – Sartomer, $I_{(3)}$ – General electric). $Ph_2I^{\oplus}$ $SbF_6^{\ominus}$ was prepared from the chloride (Fluka) by exchanging the anion and was purified by precipitating them from a solution in isopropanol by adding heptane (50% v/v). The spiropyran was prepared according to Ref. [7]. All other chemicals and solvents were obtained commercially in the highest available purity. The solvents were dried over molecular sieves 4 Å (Fluka). Diphenylanthracene was purified by vacuum sublimation. The other products were used as received.

For the Stern–Volmer measurements, a Perkin–Elmer LS 50-B fluorescence spectrometer was used. Fluorescence lifetimes were measured using a pulsed fluorometer (LIF 200, Zentrum für wissenschaftlichen Gerätebau der Akademie der Wissenschaften, Berlin (ZWG)); excitation: N_2-laser, λ=337 nm (MSG 350-S, ZWG) or a N_2-laser pumped dye laser LC 4000 (Lambda-Physik) pulse width 0.5 ns; detection: boxcar integrator; deconvolution. For a detailed description (see Ref. [8]). The system was interfaced to a computer; it was slightly modified with respect to the mathematical software. Time-resolved absorption spectroscopy was carried out in cooperation with the University of Leipzig and the Institute of Surface Modification, Leipzig.

The sensitized photolysis of the lipophilic products was carried out with visible light λ=405 nm. The use of this wavelength reduces the possibility of an unsensitized photolysis of the lipophilic products $I_{(1)}$, which shows a weak absorption up to 365 nm. The apparatus for determination of quantum yields (of the sensitizer decay) comprising an electronic actinometer [9] is described in detail in Ref. [10]. The excitation wavelengths, 365 nm and 405 nm respectively, were selected from the emission of a 200 W high pressure mercury lamp (HBO 200, Narva) with several filter combinations (365 nm: code-No.: 1602 and UVIF 365; 405 nm: code-No.: 1602 and IF 405 Hg, Carl Zeiss Jena). Moreover, the set-up was also used as irradiation source for the determination of the quantum yields of the proton formation.

The determination of the quantum yield of the proton formation takes place in the following procedure: 1 ml spiropyrane (5×10^{-3} mol/l in a solvent mixture CH_3OH/DME (1 : 1)) was added to 2 ml of the irradiated solution. The optical density of the formed dye was measured immediately after mixing. It is necessary to calibrate each system in each solvent. Advantageously, for the proton detection in DME the spiropyrane was solved in a mixture CH_3OH/DME (2 : 1). The formed dye is able to sensitize the iodonium salt photolysis (see also [11]). Therefore, one must work discontinuously and add the spiropyrane after the irradiation. As a consequence of transformation of the proton detection from nonprotic to protic solvent, several organic acids are useful for calibrations. We checked successful *p*-toluene sulfonic acid, tetrafluoro boric acid (in diethyl ether), and methane sulfonic acid. Otherwise in nonprotic solvents, the calibration requires waterfree hexafluoroantimonic acid. The plot optical density of the formed dye vs. proton concentration is linearly in a broad range. Nevertheless, the slope of the plot is a function of the solvent (in which the irradiation takes place) and the used iodonium salt concentration.

3. Results and discussion

3.1. Photolysis under inert conditions

3.1.1. Fluorescence quenching

With all our solvents, linear Stern–Volmer plots were found when the fluorescence of the sensitizer DPA was quenched by the iodonium salts $I_{(1)}$–$I_{(4)}$. From the Stern–Volmer relationship (1) the product $k_q\tau_0$ was determined. The results of the quenching are listed in Table 1. Additionally to the dynamic quenching of the fluorescence (τ_0/τ) the quenching of the fluorescence intensity (I_0/I) was carried out. The results obtained from Eq. (2) are also listed in Table 1.

$$\tau_0/\tau = 1 + k_q\tau_0[I^{\oplus}] \quad (1)$$

$$I_0/I = 1 + K^{SV}[I^{\oplus}] \quad (2)$$

where τ_0 and τ are the singlet lifetimes of the sensitizer in the absence and presence of the iodonium salt, k_q the quenching rate constant, $[I^{\oplus}]$ the concentration of the used iodonium salt, I_0 and I the fluorescence intensities in the absence and presence of the iodonium salt $I^{\oplus}$, and K^{SV} the Stern–Volmer constant.

In a given solvent the obtained $k_q\tau_0$-values are similar for $I_{(1)}$–$I_{(4)}$, and they show a systematic and consistent trend towards lower values with decreasing solvent polarity. The determined K^{SV}-values show the same trend. Overall, the results of the intensity measurements confirm the findings of the dynamic quenching. Nevertheless, in acetonitrile the

Table 1
Fluorescence quenching of DPA under argon ([DPA]=5×10^{-5} mol/l; [$I^{\oplus}$]=0...6×10^{-3} mol/l, excitation wavelength: $\lambda\approx400$ nm (dynamic measurements), respectively $\lambda=393$ nm (stationary measurements), abbreviations see text; $k_q\tau_0$, K^{SV} and K in l/mol)

Solvent	$I_{(1)}$		$I_{(2)}$		$I_{(3)}$		$I_{(4)}$	
	$k_q\tau_0/K^{SV}$	K	$k_q\tau_0/K^{SV}$	K	$k_q\tau_0$ [a]$/K^{SV}$	K	$k_q\tau_0/K^{SV}$	K
CH_3CN	90/200 (65%)	77	83/100 (17%)	— [d]	72/115 (37%)	28	92/140 (34%)	33
CH_3OH	67/117 (63%)	36	55/63 (13%)	— [d]	53/71 (25%)	16	70/72	~0
DME	28/68 (58%)	35	42/44	~0	30/42 (28%)	9	45/44	~0
Dioxane	— [b]	— [b]	— [b]	— [b]	— [b]	— [b]	23/32 (28%)	7
n-Heptane	~0/32 (100%)	32	— [c]	— [c]	— [c]	— [c]	— [c]	— [c]

[a] 337 nm.
[b] Not measured.
[c] Insoluble in this solvent.
[d] Nonlinear plot according to Eqs. (4a) and (4b).

obtained values of the intensity measurements of the salts $I_{(1)}$, $I_{(2)}$, and $I_{(4)}$ are significantly larger than the values obtained by the dynamic quenching. These results point out a static part in the fluorescence quenching, which can be observed by a complex formation in the ground state. A static part of quenching was observed for $I_{(1)}$ in all solvent used and for $I_{(4)}$ in dioxane.

Under these conditions, the quenching of the fluorescence intensity must be described by means of Eq. (3), where the ratio of the fluorescence intensity depend on [$I^{\oplus}$] in a nonlinear way. Nevertheless, such nonlinear dependence can be observed by means of high concentrations of the iodonium salt and strong K-values. At low concentrations and low *K*-values the square link of Eq. (3) is neglectable. Therefore, our observed linear dependence on I_0/I vs. [$I^{\oplus}$] is presumable a result of the poor solubility of the iodonium salts ($\leq10^{-2}$ mol/l) in the solvents used.

The equilibrium constants *K* of the complex formation can be separated from Eq. (4a), which can be obtained from Eq. (3) on division by Eq. (1) (see [12]). The equilibrium constants *K* are also summarized in Table 1. Nevertheless, the order of *K* do not fully describe the situation. Therefore, the part of the static quenching was added in the table. Interestingly, in heptane the observed overall quenching was caused only by the static part.

– Static and dynamic fluorescence quenching:

$$I_0/I = (1+K[I^{\oplus}])(1+k_q\tau_0[I^{\oplus}]) = 1+K[I^{\oplus}]+k_q\tau_0[I^{\oplus}] + Kk_q\tau_0[I^{\oplus}]^2 = 1+K^{SV}[I^{\oplus}] \quad (3)$$

with $K^{SV}=K+k_q\tau_0+Kk_q\tau_0[I^{\oplus}]$

– Static fluorescence quenching:

$$[DPA]_0/[DPA]_{free} = 1+K[I^{\oplus}] = (I_0/I)\times(\tau/\tau_0) \quad (4a)$$

where $[DPA]_0$ is the used concentration of diphenylanthracene, $[DPA]_{free}$ the concentration of free diphenylanthracene in an equilibrium, and *K* an equilibrium constant.

The results of the fluorescence quenching show that the general Scheme 1 of the electron transfer must be extended

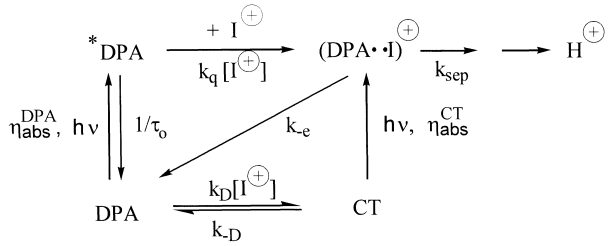

Scheme 3.

by an equilibrium between $I^{\oplus}$ and DPA in the ground state (see Scheme 3). Interestingly, changes in the UV-absorbtion were not observed in the solubility range of the iodonium salts ($\leq10^{-2}$ mol/l). Nevertheless, the formation of the ground state complex is indirect provable:

– By means of the dynamic fluorescence quenching one can observe the quenching of the lifetime of the excited sensitizer. The lifetime can be determined from Eq. (5):

$$A(t) = A_0\exp(-t/\tau) \quad (5)$$

where *A* is the fluorescence intensity by the time *t* and A_0 the fluorescence intensity by $t=0$.
– In case of an static part of quenching one observed, that the quenching of the lifetime is combined with the decrease of the A_0-value.
– By means of fluorescence quenching, such behaviour can be observed in two cases (a) by an intern filter effect of the quencher or (b) by decrease of the concentration of the excited singlet state.
– By the used irradiation wavelength (400 nm) an intern filter effect of the quencher can be excluded. Using a constant laser intensity, the decrease of A_0 results from the decrease of the ground state concentration of DPA. The order of A_0 is proportional to [DPA].
– The above discussion yields in Eq. (4b):

$$(A_0)_o/(A_0)_q = [DPA]_0/[DPA]_{free} = 1+K[I^{\oplus}] \quad (4b)$$

where $(A_0)_o$ is the order of A_0 without iodonium salt, and $(A_0)_q$ the order of A_0 with iodonium salt.

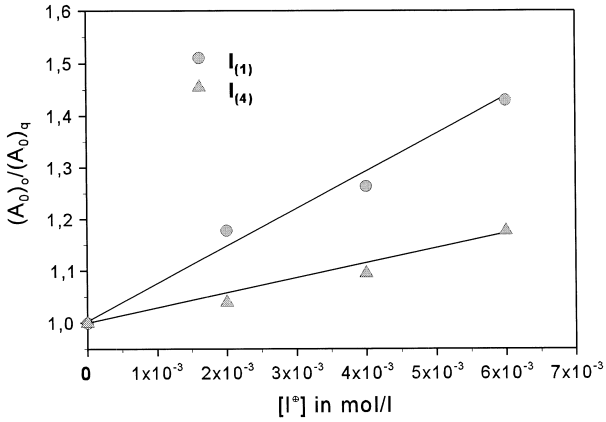

Fig. 1. Fit according to Eq. (4b) for two typical iodonium salts ([DPA]=5×10^{-5} mol/l; solvent CH_3CN; excitation wavelength: λ=400 nm).

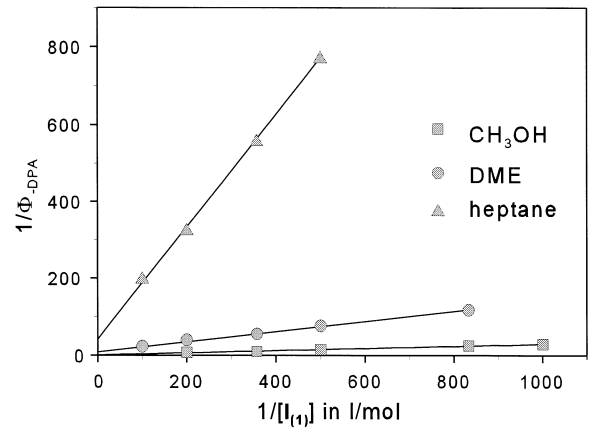

Fig. 2. Typical plots according to Eq. (7) for the lipohilic salt $I_{(1)}$ in several argon-saturated solvents ([DPA]=10^{-4} mol/l; excitation wavelength: λ=405 nm).

– The experimental check of Eq. (4a) using a constant laser intensity, in one solvent (acetonitrile) and $I_{(1)}$, and $I_{(4)}$ respectively gives K-values (75 $I_{(1)}$, and 27 $I_{(4)}$ respectively), which are similar to the value in Table 1 (see Fig. 1).

3.1.2. Sensitizer decay

The results of the fluorescence quenching shows that the general Scheme 1 of the electron transfer must be extended by an equilibrium in the ground state (see Scheme 3). Under the assumption, both DPA and CT absorb light in the same region and both compounds lead to the same cationic radical pair (the light absorption of the formed complex gives not the excited singlet state of DPA than this concentration decreases with increasing iodonium salt concentration) the kinetic modelling of Scheme 3 results in a complex expression for the quantum yield of the sensitizer decay and the quantum yield of the proton formation (see Eq. (6)). A linear relationship is obtained by inverting this equation (see Eq. (7)).

$$\Phi_{-\mathrm{DPA}} = \Phi_{\mathrm{H}^{\oplus}} = \eta_{\mathrm{abs}}^{\mathrm{DPA}}\eta_{\mathrm{q}}\eta_{\mathrm{sep}} + \eta_{\mathrm{abs}}^{\mathrm{CT}}\eta_{\mathrm{sep}} = \eta_{\mathrm{sep}}\left(\frac{B[\mathrm{I}^{\oplus}]}{1/\tau_0 + B[\mathrm{I}^{\oplus}]}\right) \tag{6}$$

with $\eta_{\mathrm{sep}}=k_{\mathrm{sep}}/k_{\mathrm{sep}}+k_{-\mathrm{e}}$; $\eta_{\mathrm{q}}=k_{\mathrm{q}}/(1/\tau_0+k_{\mathrm{q}}[\mathrm{I}^{\oplus}])$; $\eta_{\mathrm{abs}}^{\mathrm{DPA}} = [\mathrm{DPA}]_{\mathrm{free}}/[\mathrm{DPA}]_0 = 1/(1+K[\mathrm{I}^{\oplus}])$ and $\eta_{\mathrm{abs}}^{\mathrm{DPA}} + \eta_{\mathrm{abs}}^{\mathrm{CT}} = 1$; $\varepsilon^{\mathrm{CT}} \approx \varepsilon^{\mathrm{DPA}}$

$$\frac{1}{\Phi_{-\mathrm{DPA}}} = \frac{1}{\Phi_{\mathrm{H}^{\oplus}}} = \frac{1}{\eta_{\mathrm{sep}}}\left(1 + \frac{1}{\tau_0 B[\mathrm{I}^{\oplus}]}\right) = \frac{1}{\eta_{\mathrm{sep}}}\left(1 + \frac{1}{K^{\mathrm{SV}}[\mathrm{I}^{\oplus}]}\right) \tag{7}$$

where $\Phi_{-\mathrm{DPA}}$ is the quantum yield of sensitizer decay, $\Phi_{\mathrm{H}^{\oplus}}$ the quantum yield of proton formation, η_{sep} the separation efficiency of the cationic radical pair, η_{q} the quenching efficiency of the excited sensitizer by the iodonium salt, η_{abs} (indicated with DPA) the part of absorption of the free DPA, and η_{abs} (indicated with CT) the part of absorption of the formed complex, and B a complex quantity ($B=k_{\mathrm{q}}+K/\tau_0+K\ k_{\mathrm{q}}[\mathrm{I}^{\oplus}]=K^{\mathrm{SV}}/\tau_0$ (see (Eq. (3))).

Using DPA, the quantum yield of sensitizer decay $\Phi_{-\mathrm{DPA}}$ was measured as function of the iodonium salt concentration. The obtained values correlate well with Eq. (7). Typical plots according to Eq. (7) are given in Fig. 2. From the slope of the plot one can estimate K^{SV} by dividing and inverting the slope of the plot by the intercept. The K^{SV}-values, determined by dividing and inverting the slope by the intercept, are nearly identical with the independently determined values of the fluorescence quenching. Table 2 summarizes all K^{SV} and η_{sep}-values for the used lipophilic salts $I_{(1)}$–$I_{(3)}$ and the product $I_{(4)}$.The slopes of the plot according to Eq. (7) have also been compiled in Table 2.

In a given solvent these slopes are similar for all lipophilic iodonium salts. The slopes show a systematic and consistent trend towards higher values with decreasing solvent polarity. Furthermore, the solvent polarity determines also the intercept. The behaviour is similar to the unsubstituted product, where the maximal value was observed in the protic solvent methanol. Nevertheless, the effect on η_{sep} is stronger by $I_{(1)}$–$I_{(3)}$.

3.1.3. Proton formation

The importance of proton formation [13] requires the determination of the efficiency of this process. We have adapted an indicator dye method (see Scheme 4) to measure the quantum yields for proton formation [14]. The plot optical density of the formed dye vs. proton concentration (see Fig. 3) shows that the system works linearly in a broad range. We have checked the method using the known quantum yield of the direct photolysis of the lipophilic iodonium salt $I_{(1)}$ in the solvent mixture of dimethoxymethane and hexamethyldisiloxane [15]. The equality of the quantum yield of proton formation (0.29) and the quantum yield onium salt photolysis (0.30) proves that the system is useful for the proton detection.

Table 2
Results of the DPA-photolysis (Φ_{-DPA}) under argon in solvents with different polarity ([DPA]=10^{-4} mol/l; [$I^{\oplus}$]=1...10×10^{-3} mol/l, excitation wavelength: λ=405 nm (365 nm $I_{(4)}$); abbreviations see text, units: K^{SV} in l/mol; slope in mol/l))

Solvent	$I_{(1)}$			$I_{(2)}$			$I_{(3)}$			$I_{(4)}$		
	K^{SV}	η_{sep}	Slope	K^{SV}	η_{sep}	Slope	K^{SV}	η_{sep}	Slope	K^{SV}	η_{sep}	Slope
CH_3CN	230	0.25	0.017	145	0.43	0.016	138	0.33	0.022	125	0.67	0.012
CH_3OH	71	0.50	0.028	50	0.66	0.031	85	0.40	0.028	63	0.67	0.024
DME	68	0.11	0.134	35	0.25	0.114	34	0.25	0.118	32	0.56	0.056
Heptane	21	0.033	1.45	— [a]	— [a]	— [a]	— [a]	— [a]	— [a]	— [a]	— [a]	— [a]

[a] Insoluble in this solvent.

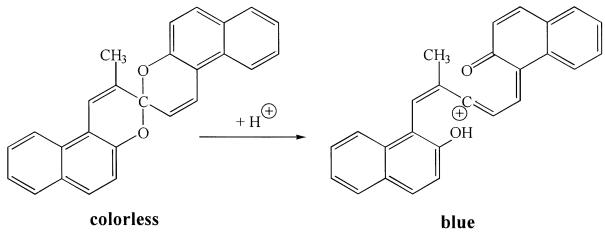

Scheme 4.

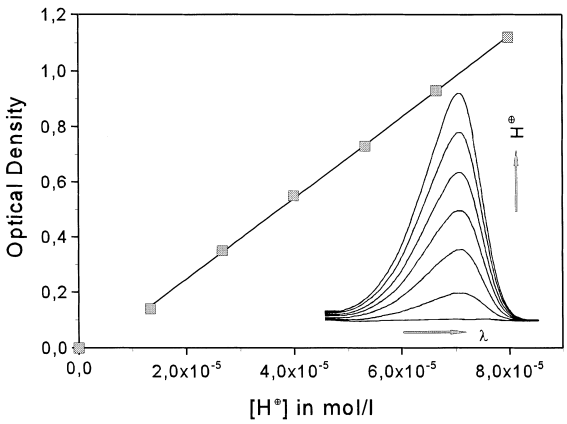

Fig. 3. Calibration of the spiropyran dye formation by addition of *p*-toluene sulfonic acid (system DPA/$I_{(3)}$/DME; [DPA]=10^{-4} mol/l; [$I_{(3)}$]=2×10^{-3} mol/l; for more details see Section 2).

Generally in acetonitrile, for all used iodonium salts linear relationships according to Eq. (7) were found. Fig. 4 shows for the two typical iodonium salts $I_{(1)}$ and $I_{(4)}$ the results of the sensitized proton formation. By means of $I_{(2)}$, $I_{(3)}$ and $I_{(4)}$, the quantum yield of proton formation is approximately the same than the quantum yield of the sensitizer photolysis. Nevertheless, for $I_{(1)}$ we found $\Phi_{H^{\oplus}} > \Phi_{-DPA}$. Coherently, the estimated value of the Stern–Volmer constant, determined by dividing and inverting the slope of the plot by the intercept, depends on the determination method (Φ_{-DPA}, $\Phi_{H^{\oplus}}$).

Curiously, the slopes of the plot are similar. Φ_{-DPA} are connected with $\Phi_{H^{\oplus}}$ by Eqs. (8) and (9). Nevertheless, these equations are empirical correlation. A kinetic scheme, which results in this correlation is unknown at this time.

$$\frac{\Phi_{-DPA}}{\eta_{abs}^{DPA}} = \Phi_{H^{\oplus}} \quad (8)$$

$$\frac{1}{\Phi_{-DPA}} = \frac{1}{\Phi_{H^{\oplus}}} + \frac{\eta_{abs}^{CT}}{\Phi_{-DPA}} \quad (9)$$

The reason for this peculiar behaviour is not fully clear at this time. However, a chain reaction as mainspring can be excluded. The kinetic modulation shows that a chain reaction has no influence on the Stern–Volmer constant when this value was determined from the slope and the intercept because a chain reaction influences the intercept and slopes in the same manner.

Nevertheless, chain reactions of proton formation were observed in the typical H-donator solvents. For an example, in MeOH chain lengths larger than 50 were observed. These findings agree with the results from Timpe and Jönsson and

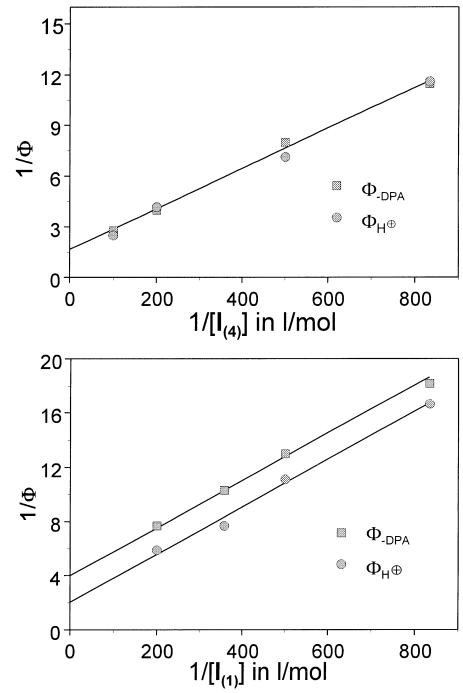

Fig. 4. Plots $1/\Phi$ vs. $1/[I\Phi]$ for $I_{(1)}$ and $I_{(4)}$ in argon-saturated CH_3CN ([DPA]=10^{-4} mol/l; excitation wavelength: λ=405 nm ($I_{(1)}$) or 365 nm ($I_{(4)}$), respectively).

suggest a secondary radical induced proton formation [5,6]. Nevertheless, the repetition of the values is difficult, because $\Phi_{H^{\oplus}}$ shows a strong dependence from the oxygen content of the solution. However, our findings show that in an air-saturated solution the chain reaction is completely quenched. Measurements of $\Phi_{H^{\oplus}}$ under air may be a good method for investigating the proton formation.

3.2. Photolysis under air and oxygen

3.2.1. Fluorescence quenching under air

Oxygen is well-known as quencher for radical reactions and excited singlet states. By means of flash photolysis experiments, we can show that oxygen quenches photoexcited DPA diffusion controlled. Moreover, the result of this quenching is DPA in the ground and DPA in the triplet state, which can be also quenched by oxygen. Fortunately our results show, that iodonium salts do not quench the triplet state of DPA. This result agrees with thermodynamical calculation, which show that electron transfer quenching of DPA by iodonium salts is feasible only in the singlet state. The results of the fluorescence quenching under air are summarized in Table 3. In a given solvent, the $k_q\tau_0$-values are similar for $I_{(1)}$–$I_{(4)}$, and they show a systematic and consistent trend towards lower values with decreasing solvent polarity. The trend is similar than under inert conditions. In a first approximation, one can expect that oxygen influences only the lifetime of the singlet state. The dynamic fluorescence quenching confirms this thesis. The determined k_q-values are nearly independent of the atmospheric conditions.

Oxygen influenced the static quenching in a indifferent way. Mostly, the influence is weak. Nevertheless, stronger effects were observed for $I_{(2)}$ and $I_{(3)}$ in acetonitrile, $I_{(1)}$ in methanol and for $I_{(4)}$ in dioxane.

Moreover, the quenching of the fluorescence intensity using $I_{(1)}$ and $I_{(4)}$ confirm the own results. Nevertheless, in acetonitrile the obtained values are some times larger than the so far published values [3]. We would ascribe this to the use of different charges of the products $I_{(1)}$ and $I_{(4)}$. The feasible check using $I_{(1)}$ confirms this thesis.

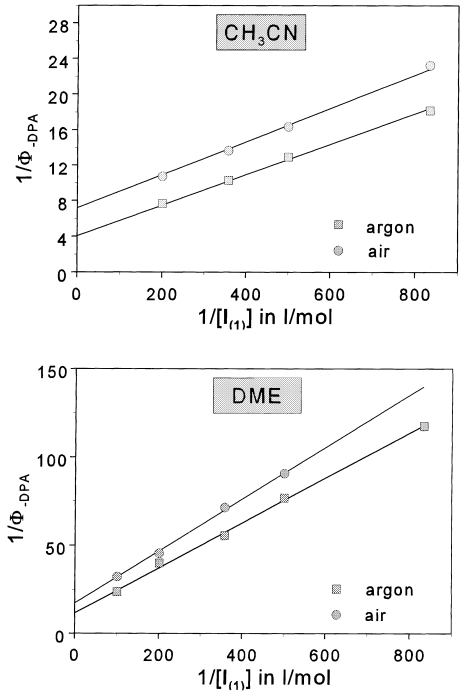

Fig. 5. Influence of the atmospheric conditions on the plot $1/\Phi_{-DPA}$ vs. $1/[I_{(1)}]$ in two typical solvents ([DPA]=10^{-4} mol/l; excitation wavelength: λ=405 nm).

3.2.2. Sensitizer decay under air and oxygen

Under air, the quantum yield of sensitizer decay Φ_{-DPA} was measured also as function of the iodonium salt concentration. The obtained values satisfy Eq. (7). Typical plots are shown in the Fig. 5. The slopes show a systematic and consistent trend towards higher values with decreasing solvent polarity. Furthermore, the solvent polarity also determines the intercept relative to η_{sep}. The behaviour is similar to the results under inert conditions (see Table 4).

Nevertheless, the estimated K^{SV}-values obtained by dividing and inverting the slope of the plot by the intercept are larger (with exception of the results in methanol) than the constants determined independently by fluorescence quenching. This fact is incompatible with the used scheme of electron transfer and the assumption that oxygen influ-

Table 3
Fluorescence quenching of DPA under air ([DPA]=5×10^{-5} mol/l; [$I^{\oplus}$]=0...6×10^{-3} mol/l, excitation wavelength: $\lambda\approx$400 nm (dynamic measurements), respectively λ=393 nm (stationary measurements), abbreviations see text; $k_q\tau_0$, K^{SV} and K in l/mol)

Solvent	$I_{(1)}$		$I_{(2)}$		$I_{(3)}$		$I_{(4)}$	
	$k_q\tau_0/K^{SV}$	K	$k_q\tau_0/K^{SV}$	K	$k_q\tau_0$ [a]/K^{SV}	K	$k_q\tau_0/K^{SV}$	K
CH_3CN	65 [b]/217 (70%)	110	55/93 (41%)	29	57/60	~0	75/125 (40%)	36
CH_3OH	50/67 (26%)	16	42/42	0	35/38	~0	53/54	~0
DME	16/35 (46%)	18	19/20	~0	30/30	0	27/32	~0
Dioxane	— [c]	— [c]	— [c]	— [c]	— [c]	— [c]	5/32 (84%)	
n-Heptane	~0/22 (100%)	22	— [d]	— [d]	— [d]	— [d]	— [d]	— [d]

[a] 337 nm (N_2-Laser).
[b] 58 uses the old charge of $I_{(1)}$.
[c] Not measured.
[d] Insoluble in this solvent.

Table 4
Results of the DPA-photolysis (Φ_{-DPA}) under air in solvents with different polarity ([DPA]=10^{-4} mol/l; [$I^{\oplus}$]=1...10×10^{-3} mol/l, excitation wavelength λ=405 nm; abbreviations see text, units: K^{SV} in l/mol; slope in mol/l)

Solvent	$I_{(1)}$ [a]			$I_{(2)}$			$I_{(3)}$			$I_{(4)}$ [b]		
	K^{SV}	η'_{sep}	Slope	K^{SV}	η'_{sep}	Slope	K^{SV}	η'_{sep}	Slope	K^{SV}	η'_{sep}	Slope
CH_3CN	376	0.14	0.019	181	0.25	0.022	146	0.18	0.038	215	0.33	0.014
CH_3OH	68	0.40	0.037	54	0.45	0.041	95	0.25	0.042	80	0.40	0.031
DME	106	0.063	0.150	76	0.12	0.11	68	0.10	0.144	52	0.25	0.078
Heptane	32	0.02	1.54	— [c]	— [c]	— [c]	— [c]	— [c]	— [c]	— [c]	— [c]	— [c]

[a] Results with uncorrected values in heptane: K^{SV}=234; η_{sep}=0.007; slope=0.61.
[b] Irradiation wavelength λ=365 nm.
[c] Insoluble in the solvent.

ences only the lifetime of the singlet state. O_2-bleaching of DPA as reason of this effect can be excluded in acetonitrile, and dimethoxyethane, because the quantum yield of O_2-bleaching of DPA ($\Phi_{-DPA}(O_2)$ is in the order of 10^{-3}. With exception of the results in heptane this value is 1–2 orders of magnitude lower than the lowest measured Φ_{-DPA}-value. Nevertheless in heptane, the O_2-bleaching of DPA is not in agreement with the measured Φ_{-DPA}-values. The corrected quantum yields (Φ_{-DPA}(corrected)=Φ_{-DPA}(measured) $-\Phi_{-DPA}(O_2)$) satisfy Eq. (7). Moreover, the K^{SV}-value, determined by means of Eq. (7), are nearly identical with the independently determined value of the fluorescence quenching.

Fig. 5 shows, that oxygen influences both the slope of the plot and the intercept. Moreover, the oxygen effect is stronger on the intercept than on the slope. Only in methanol and *n*-heptane it is observed that slope and intercept of the plot varies approximately in the same manner. Consequently, in this solvent similar Stern–Volmer constants were obtained with both methods.

$$^{*}DPA + O_2 \xrightarrow{k_{des}} DPA + products \quad (11)$$

$$(DPA..I)^{\oplus} + O_2 \xrightarrow{k_{ox}} DPA + products \quad (12)$$

From Fig. 5 (see also Table 3) one can derive that oxygen influences intercept and slope. The used scheme of the electron transfer (Scheme 3) presents two possibilities of the attack of oxygen, (a) the photoexcited DPA (*DPA) and (b) the cationic radical pair (DPA. .I)$^{\oplus}$ (see Eqs. (11) and (12)). The quenching of the excited state yields in a reduced lifetime of the sensitizer, and the quenching of the radical pair yields in a reduced η_{sep}-value, than a third deactivation way is added to the scheme. Nevertheless, this oxygen quenching of the radical pair and of the excited state results in Eq. (14), where slope and intercept were influenced in the same manner. The obtained strong differences in the determinations of the Stern–Volmer constant cannot be explained with this type of oxygen quenching.

$$\Phi_{-DPA} = \Phi_{H^{\oplus}} = \eta_{abs}^{DPA} n_q \eta'_{sep} + \eta_{abs}^{CT} \eta'_{sep} = \eta'_{sep}\left(\frac{B'[I^{\oplus}]}{1/\tau_0 + k_{des}[O_2] + B'[I^{\oplus}]}\right) \quad (13)$$

with $\eta'_{sep} = k_{sep}/(k_{sep} + k_{-e} + k_{ox}[O_2])$

$$\frac{1}{\Phi_{-DPA}} = \frac{1}{\Phi_{H^{\oplus}}} = \frac{1}{\eta'_{sep}}\left(1 + \frac{1}{K_{air}^{SV}[I^{\oplus}]}\right) \quad \text{with } K_{air}^{SV} = \left(\frac{B'}{1/\tau_0 + k_{des}[O_2]}\right) \quad (14)$$

$$\Phi_{-DPA} = \Phi_{H^{\oplus}} = \eta_{abs}^{DPA}\eta_q\eta_e\eta'_{sep} + \eta_{abs}^{CT}\eta'_{sep} = \eta'_{sep}\left(\frac{C[I^{\oplus}]}{1/\tau_0 + k_{des}[O_2] + \eta_{oxy}k_q[I^{\oplus}] + C[I^{\oplus}]}\right) \quad (15)$$

with $\eta_e = k_e/(k_e + k_{oxy}[O_2])$; and $\eta_{oxy} = k_{oxy}[O_2]/(k_e + k_{oxy}[O_2])$

$$\frac{1}{\Phi_{-DPA}} = \frac{1}{\Phi_{H^{\oplus}}} = \frac{1}{\eta'_{sep}}\left(1 + \frac{1/\tau_0 + k_{des}[O_2]}{C[I^{\oplus}]} + \frac{\eta_{oxy}k_q}{C}\right) \quad (16)$$

where B' and C are complex quantities ($B' = k_q + K(1/\tau_0 + k_{des}[O_2]) + Kk_q[I^{\oplus}]$; $C = \eta_e k_q + K(1/\tau_0 + k_{des}[O_2]) + Kk_q[I^{\oplus}]$).

All experiments show, that our kinetic Scheme must by extended by a second intermediate, which can also be quenched by oxygen (see Scheme 5). The kinetic modelling of this Scheme results in a complex expression, which gives in the inverted form a linear correlation between the inverse quantum yield and the inverse iodonium salt concentration, which differ from the equation under inert condition by an absolute value and by a different slope. This absolute value is the cause of the stronger effect of oxygen on the intercept than on the slope.

Two limiting cases can be discussed under air:

1. Oxygen quenches only the excited sensitizer and the intermediate ($k_{ox}[O_2] \ll (k_{sep} + k_{-e})$). The oxygen quenching of the intermediate is <30% ($\eta_{oxy} \leq 0.3$ corresponds to the quenching of the singlet state). This assumption results in identical separation efficiencies under air and inert conditions. Moreover, the slope of the plot, is in a first approximation the inverse Stern–Volmer constant under air.

$$\frac{1}{\Phi_{-DPA}} = \frac{1}{\Phi_{H^{\oplus}}} \approx \frac{1}{\eta_{sep}}\left(1 + \frac{1}{K_{air}^{SV}[I^{\oplus}]} + \frac{\eta_{oxy}k_q}{C}\right) \quad (16a)$$

2. Oxygen quenched only the excited sensitizer and the cationic radical pair ($\eta_{oxy} \approx 0$ and $k_{ox}[O_2] \approx ((k_{sep} + k_{-e}))$.

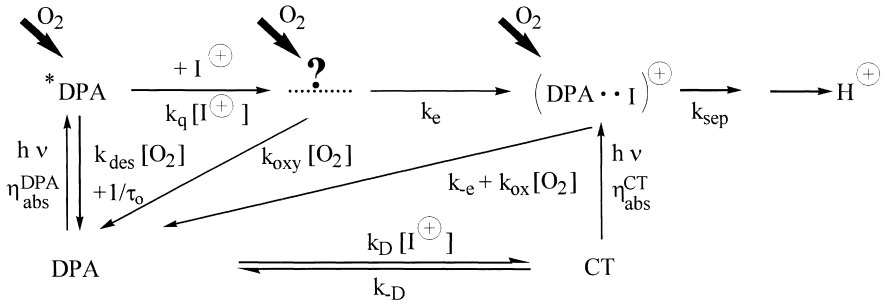

Scheme 5.

This oxygen quenching of the radical pair and of the excited state results in Eq. (14), where slope and intercept were influenced in the same manner.

Mostly, the oxygen effect is a mixture of both. In acetonitrile, the sensitizer decay can be described using Eq. (16a), so that the low differences of K^{SV} under air and inert conditions result in nearly parallel plots. Nevertheless, the intercept of the plot differ for both systems. Overall, this behaviour results in a wrong determination of K^{SV} by dividing and inverting the slope of the plot by the intercept. Moreover, in methanol and *n*-heptane the sensitizer decay can be described with Eq. (14).

Nearly parallel plots in acetonitrile show that oxygen quenches in acetonitrile only via the excited singlet state. Moreover, the oxygen quenching of the unknown intermediate and the singlet state are of the same order. Oxygen may quench almost completely in this manner so that the product of η_q and η_e is <0.06 (η_q<0.25 indicates that the O_2-quenching of *DPA is >75% under the assumption that $\eta_q \approx \eta_e$). Under this assumption, the reaction scheme can be simplified so that the photochemistry of the system is reduced to the photochemistry of the CT complex. The kinetic modelling of this simplified scheme results in Eq. (17).

The experimental proof using $I_{(1)}$ and $I_{(4)}$ shows that the used model and assumptions are justified (see Fig. 6). The plot gives directly the equilibrium constant of the complex formation (K=120 ($I_{(1)}$), and 38 ($I_{(4)}$) respectively). The obtained values for the equilibrium constant agree with the fluorescence quenching results. Moreover, the estimated values for η_{sep} (0.2 ($I_{(1)}$), and 0.67 ($I_{(4)}$) respectively) show that the oxygen quenching of the cationic radical pair can be neglected in acetonitrile.

$$\frac{1}{\Phi_{-\mathrm{DPA}}} = \frac{1}{\Phi_{\mathrm{H}^{\oplus}}} \approx \frac{1}{\eta_{sep}}\left(1 + \frac{1}{K[\mathrm{I}^{\oplus}]}\right) \tag{17}$$

3.2.3. Proton formation

Generally, linear relationships for all solvents and iodonium salts used were found, when the reciprocal quantum yield of proton formation was plotted against the reciprocal iodonium salt concentration. In Fig. 7 for two typical solvents a plot $1/\Phi_{H^{\oplus}}$ vs. $1/I_{(4)}$ is given. The figure shows, that under air the quantum yield of proton formation is approximately the same than the quantum yield of the sensitizer

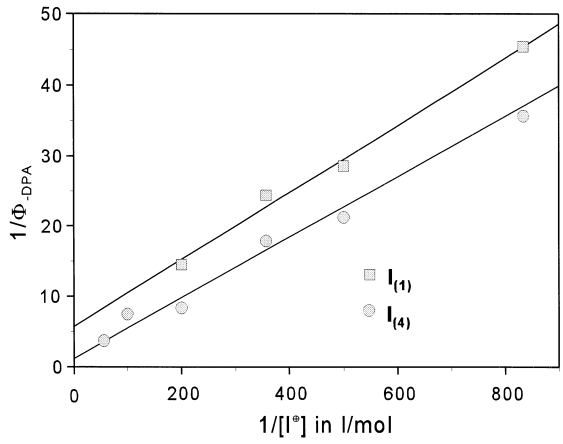

Fig. 6. Plots $1/\Phi_{-\mathrm{DPA}}$ vs. $1/[\mathrm{I}^{\oplus}]$ for $I_{(1)}$ and $I_{(4)}$ in oxygen-saturated CH_3CN ([DPA]=10^{-4} mol/l; excitation wavelength: λ=405 nm ($I_{(1)}$) or 365 nm ($I_{(4)}$), respectively).

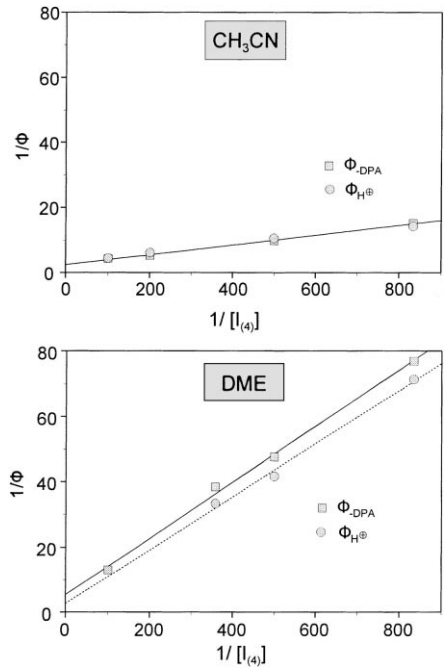

Fig. 7. Plots $1/\Phi$ vs. $1/[I_{(4)}]$ in two air-saturated solvents ([DPA]=10^{-4} mol/l; excitation wavelength: λ=365 nm).

Table 5
Results of the sensitized proton formation ($\Phi_{H^{\oplus}}$) under air in solvents with different polarity ([DPA]=10^{-4} mol/l; [$I^{\oplus}$]=1...10×10^{-3} mol/l, excitation wavelength λ=405 nm; abbreviations see text, units: K^{SV} in l/mol; slope in mol/l)

Solvent	$I_{(1)}$			$I_{(2)}$			$I_{(3)}$			$I_{(4)}$ [a]		
	K^{SV}	η'_{sep}	Slope	K^{SV}	η'_{sep}	Slope	K^{SV}	η'_{sep}	Slope	K^{SV}	η'_{sep}	Slope
CH_3CN	125 [b]	0.40	0.020	117 [b]	0.45	0.019	146	0.18	0.038	215	0.33	0.014
CH_3OH	77	0.37	0.035	54	0.45	0.041	95	0.25	0.042	80	0.40	0.031
DME	206 [b]	0.11	0.044	145 [b]	0.13	0.053	68 [c]	0.20	0.074	52	0.25	0.078
Heptane	23 [c]	0.10	0.430	— [d]	— [d]	— [d]	— [d]	— [d]	— [d]	— [d]	— [d]	— [d]

[a] Irradiation wavelength λ=365 nm.
[b] The differences between Tables 4 and 5 result from $\Phi_{H^{\oplus}} > \Phi_{-DPA}$, where intercept and slope of Eq. (7) were influenced in a different manner.
[c] $\Phi_{H^{\oplus}} > \Phi_{-DPA}$, intercept and slope of Eq. (7) were influenced in the same manner.
[d] Insoluble in the solvent.

photolysis ($\Phi_{-DPA}\approx\Phi_{H^{\oplus}}$) (see also Table 5). Nevertheless, in DME the proton formation is a little bit larger than the sensitizer decay.

Fig. 8 summarizes the results of the sensitized proton formation using the lipophilic iodonium salt $I_{(1)}$. The figure shows that the behaviour of the lipophilic salt differs from the unsubstituted product. Only in methanol is the quantum yield of proton formation approximately the same as the quantum yield of the sensitizer photolysis. In all other solvents, the quantum yield of the proton formation is larger than the quantum yield of the sensitizer photolysis. The reason for this peculiar behaviour is not fully clear at this time. The discrepancies found between $\Phi_{H^{\oplus}}$ and Φ_{-DPA} shows that the complex kinetic scheme cannot fully describe the system. Oxygen as mainspring for this effect can be excluded as this effect was found under argon, air and oxygen.

The photochemical behaviour of $I_{(2)}$ is similar to $I_{(1)}$ (see Table 5). One can observe the same trends: (a) in acetonitrile (nearly parallel plots from $1/\Phi_{-DPA}$ and $1/\Phi_{H^{\oplus}}$ vs. $1/[I_{(2)}]$); (b) in methanol ($\Phi_{-DPA}\approx\Phi_{H^{\oplus}}$); and (c) in dimethoxyethane the K^{SV}-values (determined from the plot $1/\Phi_{-DPA}$, and

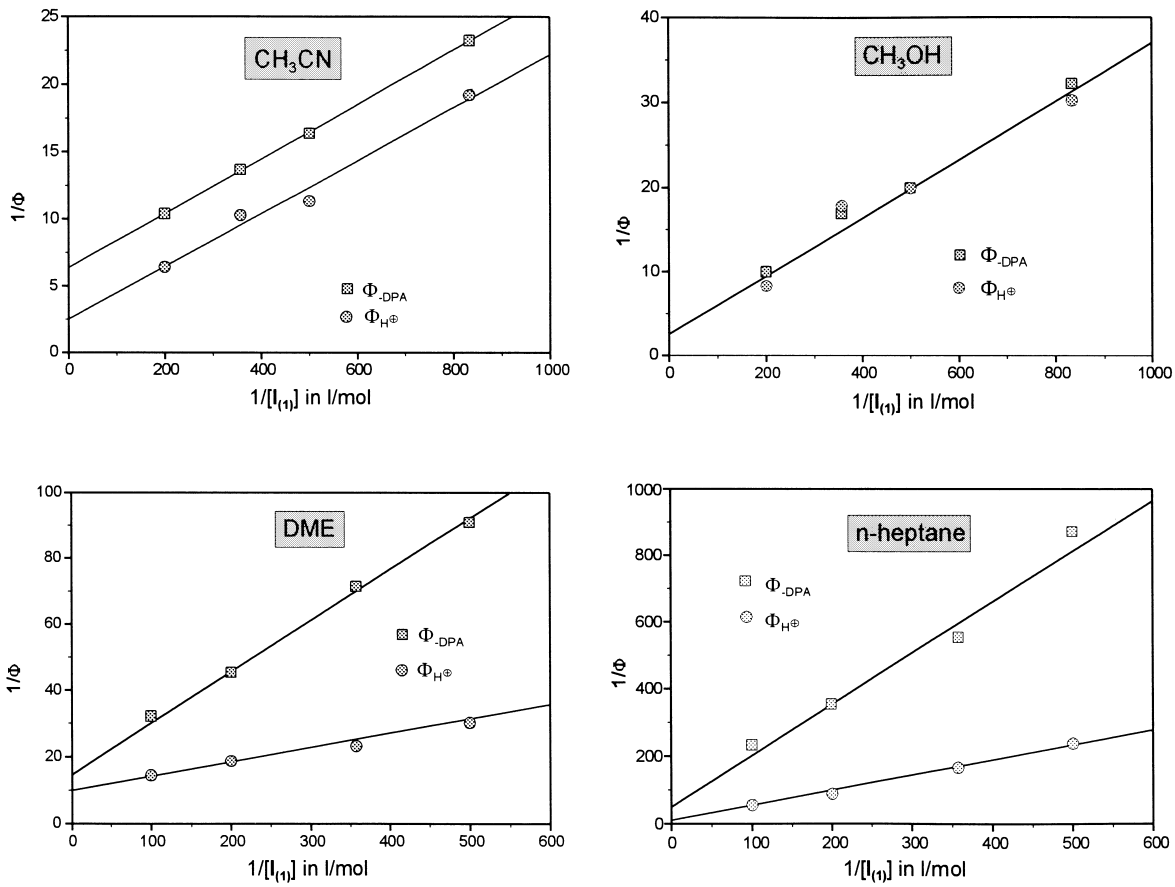

Fig. 8. Plots $1/\Phi$ vs. $1/[I_{(1)}]$ in air-saturated solvents ([DPA]=10^{-4} mol/l; excitation wavelength: λ=405 nm).

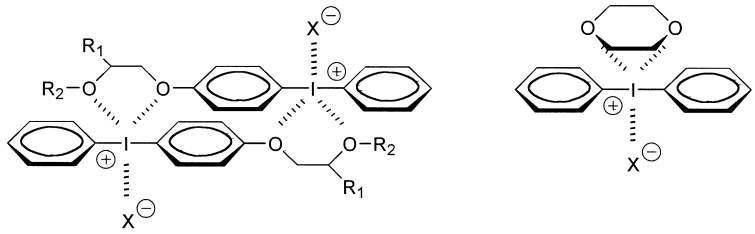

Scheme 6.

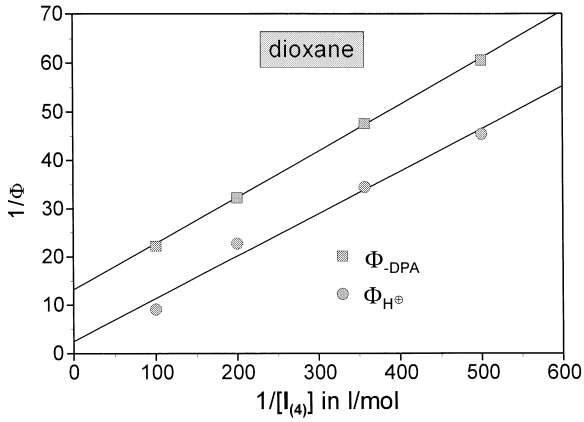

Fig. 9. Plots $1/\Phi$ vs. $1/[I_{(4)}]$ in air-saturated dioxane ([DPA]=10^{-4} mol/l; excitation wavelength: λ=365 nm).

$1/\Phi_{H^{\oplus}}$ respectively vs. $1/[I_{(2)}]$) differ by a factor 2. The comparison of the obtained results show that $I_{(1)}$ and $I_{(2)}$, which use a similar substituent with an ethylene glycol structure, give similar photochemical results.

Contrary to these findings is the behaviour of $I_{(3)}$. The claimed equality of Φ_{-DPA} and $\Phi_{H^{\oplus}}$ was found in acetonitrile and methanol. Moreover, the $k_e\tau$-values determined from the plot $1/\Phi_{-DPA}$ relative to $1/\Phi_{H^{\oplus}}$ vs. $1/[I_{(3)}]$ are equal. The photochemical behaviour of $I_{(3)}$ (having no ethylene glycol structure) is similar to $I_{(4)}$. Presumable, the observed nonequivalence of the Φ-values for $I_{(1)}$ and $I_{(2)}$ in acetonitrile, is an effect of the self-solvatisation of the lipophilic iodonium salts (see Scheme 6). Moreover, the nonequivalence of the quantum yields is combined with the emergence of a CT complex. The effect of such special solvatisation ($\Phi_{H^{\oplus}} > \Phi_{-DPA}$) was also observed for $I_{(4)}$ in dioxane and in mixtures of acetonitrile and dioxane, where a complex was also observed (see Fig. 9). Moreover, the fact that traces of water (or protic solvents, which should destroy such self-solvatisation structures) cause an equivalence of the Φ-values support this thesis.

4. Conclusions

In this work, the photosensitized proton formation of one experimental and two commercial lipophilic iodonium salts using DPA as sensitizer in solvents of different polarity was studied. Additionally, the sensitized proton formation from $Ph_2I^{\oplus}$ $SbF_6^{\oplus}$ was studied to compare the results in these solvents with those from the lipophilic iodonium salts.

The photoinduced electron transfer of DPA was investigated by fluorescence quenching, and measurements of the quantum yields of sensitizer decay or of the proton formation, respectively. As has been shown, under these circumstances the quenching mechanism is an electron transfer to give the radical cation of the sensitizer and the neutral radical of the onium salt. Energy-transfer sensitization is precluded by thermodynamics in these systems. In a solvent of lower polarity such as dimethoxyethane, the quenching rate constant is still about a third of the value in acetonitrile; the quantum yields of sensitizer decay are decreased by about the same factor.

Besides the dynamic part, the fluorescence results also point out a static part in the fluorescence quenching, which can be explained by a complex formation in the ground state. The part of the static quenching depends on the solvent and the iodonium salt used. Interestingly, in heptane the observed overall fluorescence quenching was caused only by the static part. So the results of the fluorescence quenching show that the general scheme of the electron transfer must be extended by an equilibrium in the ground state and a CT-complex formation.

Moreover, both compounds (DPA, CT complex) absorb light in the same region. Fortunately, the photochemistry of both products yields in the same intermediate, the cationic radical pair. Nevertheless, the formation of this cationic radical pair occurs on different pathways. Mostly, the observed photochemistry is a mixture of the photochemistry of the CT complex and of free DPA. In heptane the photochemistry of the system is reduced to the photochemistry of the CT complex.

Both reaction pathways show a different affinity towards oxygen. Oxygen ($[O_2]>10^{-2}$ mol/l) quenches via the excited DPA (*DPA) almost completely. Moreover, the results of the oxygen quenching of the photochemistry show that a second unknown intermediate exist between *DPA and the cationic radical pair. On the other hand, the pathway over the CT complex is nearly independent on the oxygen content. Under high oxygen concentration, the photochemistry of the system is also reduced to the photochemistry of the CT complex.

The initiating species of such an initiator system, the protons, are formed in a consecutive reaction from the cationic radical pair. Moreover, the proton formation is

connected by the consumption of the sensitizer. Chain reactions of proton formation were observed in the typical H-donator solvents. For example, in MeOH chain lengths larger than 50 were observed. However, our findings show that in an air-saturated solution the chain reaction is completely quenched. Under air the quantum yield of proton formation is comparable to the quantum yield of the sensitizer photolysis ($\Phi_{-\mathrm{DPA}} \approx \Phi_{\mathrm{H}^{\oplus}}$).

Nevertheless, in several cases one can observe $\Phi_{\mathrm{H}^{\oplus}} > \Phi_{-\mathrm{DPA}}$. Presumable, the observed nonequivalence of the Φ-values is an effect of a special solvatisation of the iodonium salts. Moreover, the nonequivalence of the quantum yields is combined with the emergence of a CT complex.

Acknowledgements

The authors thank for the financial and material support by the Deutsche Forschungsgemeinschaft and by Wacker-Chemie, Burghausen. Special thank also to Dr. W. Knolle (Institut für Oberflächenmodifizierung, Leipzig) and Dr. R. Hermann (Univerisität Leipzig) for help by the triplet quenching experiments.

References

[1] (a) J.V. Crivello, in: J.P. Fouassier, J.F. Rabek (Eds.), Radiation Curing in Polymer Science and Technology, vol. 2, , Elsevier, London, 1993, pp. 435–471; (b) M.R.V. Sahyun, R.J. DeVoe, P.M. Olofson, in: J.P. Fouassier, J.F. Rabek (Eds.), Radiation Curing in Polymer Science and Technology, vol. 2, Elsevier, London, 1993, pp. 505–527; (c) N.P. Hacker, in: J.P. Fouassier, J.F. Rabek (Eds.), Radiation Curing in Polymer Science and Technology, vol. 2, Elsevier, London, 1993, pp 473–504.

[2] A. Kunze, U. Müller, K. Tittes, J.-P. Fouassier, F. Morlet-Savary, J. Photochem. Photobiol. A: Chem. 110 (1997) 115–122.

[3] G. Eckert, M. Goez, B. Maiwald, U. Mller, Ber. Bunsenges. Phys. Chem. 100 (1996) 1191–1198.

[4] S. Murov, I. Carmichael, G.L. Hug, Handbook of Photochemistry, Marcel Dekker, Inc. New York, Basel, Hong Kong, 2nd edn., 1993.

[5] H.-J. Timpe, V. Schikowsky, J. Prakt. Chem. 331 (1989) 447–460.

[6] P.E. Sundell, S. Jönsson, A. Hult, J. Polym, Sci.: Part A: Polym. Chem. 29 (1991) 1535–1543.

[7] P. Apprijou, C. Trebaul, J. Brelivet, F. Garnier, R. Guglielmetti, Bull. Soc. Chim. 1976, pp. 2039–2046.

[8] H.G.O. Becker, G. Israel, J. Prakt. Chem. 327 (1985) 411–421.

[9] H. Baumann, H. Behrmann, H. Jahnke, W. Ortmann, G. Waldmann, J. Signalaufzeichnungsmaterialien 11 (1983) 385–394.

[10] H. Baumann, W. Lindenlaub, H.-J. Timpe, J. Prakt. Chemie 320 (1978) 825–839.

[11] Y. Ren, W.F. Jager, D.C. Neckers, Macromolecules 29 (1996) 3751–3757.

[12] H.G.O. Becker, H. Böttcher, F. Dietz, D. Rehorek, G. Roewer, K. Schiller, H.-J. Timpe, Einführung in die Photochemie, H.G.O. Becker (Eds.), Deutcher Verlag der Wissenschaften, Berlin, 1991.

[13] U. Müller, A. Kunze, Ch. Herzig, J. Weis, Organosilicon Chemistry III - From Molecules to Materials. N. Auner, J. Weis (Eds.), WILEY-VCH, Weinheim, 1997, pp. 594–604.

[14] U. Müller, A. Utterodt, J. Inf. Recording, 24 (1998) 159–164.

[15] U. Müller, A. Kunze, B. Mießbach, unpublished results.